Solid State Communications 278 (2018) 24–30

Contents lists available at ScienceDirect

Solid State Communications

journal homepage: www.elsevier.com/locate/ssc

Communication

# Gate tunable Kondo effect in magnetic molecule decorated graphene

Baoming Yan [a,b], Xinqi Li [a,b], Jiaji Zhao [a,b], Zhenzhao Jia [a,b], Fangdong Tang [c], Zhihong Zhang [a,b], Dapeng Yu [a,b], Kaihui Liu [a,b], Liyuan Zhang [c,**], Xiaosong Wu [a,b,*]

[a] State Key Laboratory for Artificial Microstructure and Mesoscopic Physics, Peking University, Beijing, 100871, China
[b] Collaborative Innovation Center of Quantum Matter, Beijing, 100871, China
[c] Department of Physics, Southern University of Science and Technology of China, Shenzhen, 518055, China

ARTICLE INFO

Communicated by E.Y. Andrei

*Keywords:*
Graphene with Cobalt(II) phthalocyanine molecule decoration
Kondo effect
Spin-flip scattering
*In situ* deposition

ABSTRACT

The Kondo effect is one of the most widely studied many-body phenomena. Magnetic impurity decorated graphene is predicted to exhibit the Kondo effect with intriguing properties. Here we study the Kondo effect in Cobalt(II) phthalocyanine magnetic molecule decorated graphene by low temperature transport measurements. Spin-flip scattering and a logarithmic increase of resistance are observed, which confirms the Kondo effect. At a high carrier density, Kondo screening persists up to 20 K, suggesting a strong coupling between Dirac electrons and local magnetic moments of molecules. Decreasing the carrier concentration by a gate voltage results in a strong suppression of Kondo screening. Such tuning of Kondo screening can be used to turn on/off the local moment. Our results demonstrate a new Kondo system based on graphene. The significant gate tunability of the system may be used in spintronics.

## 1. Introduction

The Kondo effect [1], a manifest of the interaction between localized magnetic moments and itinerant conduction electrons, is the most widely studied many-body phenomenon in condensed-matter physics [2,3]. The result is that the magnetic moment is screened below a temperature $T_K$ by the formation of a many-body singlet [4]. This very effect has provided significant insight into understanding strongly correlated systems, such as heavy-fermion materials [5–7] and high-temperature superconductors [8,9]. Recently, the Kondo effect of Dirac electrons in graphene and other materials has been predicted to exhibit intriguing properties compared with conventional metals [10–17]. Moreover, the ability to gate graphene enables investigation on the influence of the density of states (DOS), which is not possible in conventional metals [18,19]. Interestingly, at the Dirac point where the DOS vanishes, Kondo screening can be tuned off. Consequently, a quantum phase transition may occur, which was first studied in unconventional superconductor [20].

In light of above predictions, various magnetic-impurity/graphene systems have been studied [21–28]. The prerequisite of such studies is introduction of local moments, which has been achieved mainly by lattice vacancies or chemisorption. However, these defects also introduce resonance states at the Dirac point, hence a diverging DOS [29,30] (see Fig. S1 in Supplementary Materials). So, Kondo screening cannot be turned off [26,31]. In this paper, we introduce local moments by *in situ* deposition of Cobalt(II) phthalocyanine (CoPc) molecules, which is expected to be less intrusive to the Dirac band structure due to their physisorption nature [26,31]. Pronounced spin-flip scattering and a logarithmic temperature dependence of resistance are observed, both of which are evidence of the Kondo effect. Moreover, the gate dependence of the Kondo effect suggests strong suppression of Kondo screening at the Dirac point. Our experiment demonstrates graphene as a highly tunable system for studying the Kondo physics. The ability to turn on/off Kondo screening also provides a means to electrically control the spin coherence, which may be useful in spintronics [32].

## 2. Results and discussion

To obtain an ultra clean surface, a shadow mask method was used to fabricate graphene devices (Fig. 1(a)) instead of the conventional e-beam lithography. CoPc molecule (see the inset of Fig. 1(b)) decoration was carried out by *in situ* thermal deposition in a dilution refrigerator (more details in Fig. S2(e)). The samples are expected in ultra high vacuum owing to the strong cryopumping effect of the vacuum can, which

* Corresponding author. State Key Laboratory for Artificial Microstructure and Mesoscopic Physics, Peking University, Beijing, 100871, China.
** Corresponding author.
*E-mail addresses:* zhangly@sustc.edu.cn (L. Zhang), xswu@pku.edu.cn (X. Wu).

https://doi.org/10.1016/j.ssc.2018.05.001
Received 7 November 2017; Received in revised form 22 December 2017; Accepted 1 May 2018
Available online 9 May 2018

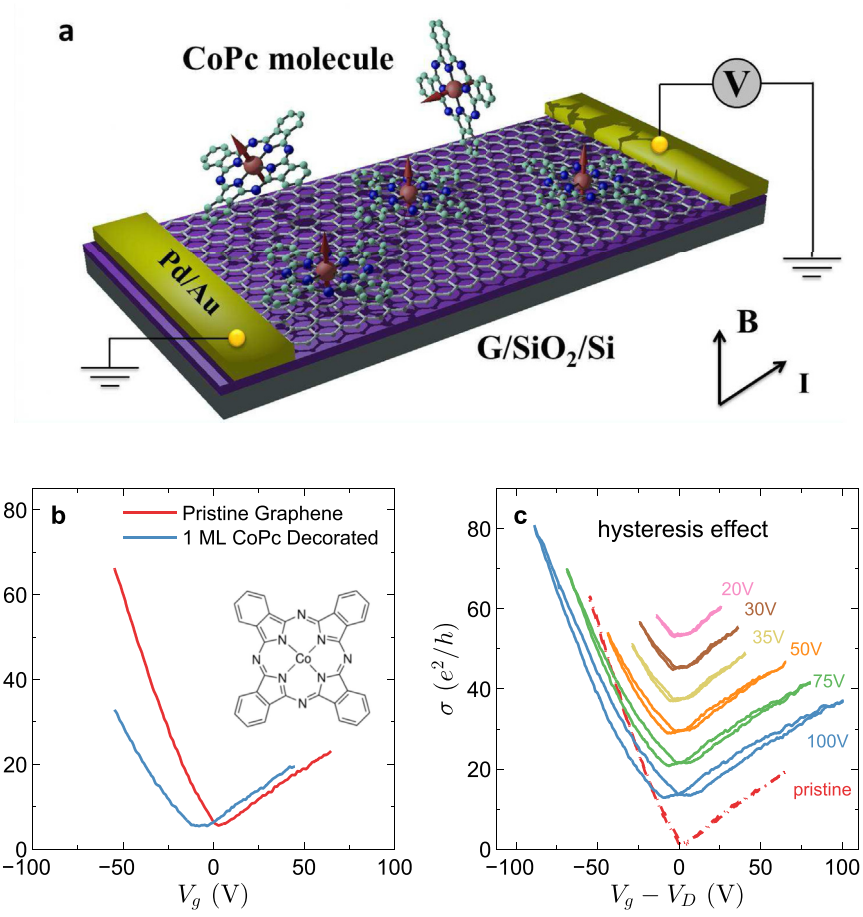


**Fig. 1.** (a) Schematic diagram for graphene device. Contacts are made of Pd/Au, and CoPc molecules are deposited *in situ* during electrical measurement. (b) Conductivity versus gate voltage for graphene before (red solid line) and after CoPc molecule deposition (blue solid line). Inset: the molecular diagram of CoPc. After a monolayer coverage of CoPc, there is a slight shift of the Dirac point, about 10 V, corresponding to an electron doping of $0.0075e/nm^2$. (c) Hysteresis effect in conductivity versus gate voltage at different voltage sweeping amplitudes. The curves are shifted in $y$ for clarity. Hysteresis, which was not observed for pristine graphene (red dashed line), appears after CoPc decoration, and becomes larger as the sweeping amplitude increases. (For interpretation of the references to colour in this figure legend, the reader is referred to the Web version of this article.)

is immersed in liquid helium. The sample temperature was maintained below 20 K throughout deposition and measurements, in order to suppress diffusing and clustering of CoPc molecules on graphene (for the influence of temperature, see Fig. S3). After the samples were cooled down to helium temperature, current annealing (current density was 0.2 mA/μm) was performed to remove possible gas adsorption. Electrical measurements were performed by a standard low-frequency lock-in technique.

The gate voltage dependence of conductivity is displayed in Fig. 1(b). For pristine graphene, the Dirac point locates near zero gate voltage, indicating a clean surface with little impurity doping. After deposition of a monolayer CoPc, the Dirac point is slightly shifted to the left (negative gate voltage) by ~10 V, indicating ionization of CoPc molecules. The shift is much smaller than that in the case of calcium deposition [33]. It is estimated that on average each CoPc molecule donates about 0.017 electron charge, supposing the average distance between molecules is 1.5 nm in monolayer [34]. Since the first ionization of CoPc removes an electron from the phthalocyanine $a_{1u}$ orbital, the spin state of $Co^{2+}$ is expected to remain at $S = 1/2$ [35]. The hole mobility decreases from 4300 $cm^2/V{\cdot}s$ to 2700 $cm^2/V{\cdot}s$ after CoPc deposition. Meanwhile, a hysteresis in the gate dependence appears, as shown in Fig. 1(c). The hysteresis is independent of the sweeping rate and becomes stronger as the gate voltage sweeps higher. It is in agreement with a charging effect [25,36].

The CoPc molecule contains a $Co^{2+}$ ion with a spin of $S = 1/2$ [37,38]. The question is whether the magnetic moment can couple to Dirac electrons in graphene. We look for transport evidence of the coupling, particularly related to spin-flip scattering. Weak localization, a phase coherent transport effect, has been one of the most important tools for extracting the spin-flip scattering rate. The phase coherence of electron leads to a quantum correction to the resistance, which has a characteristic magnetic field dependence. Spin-flip scattering, on the other hand, leads to a reduction of the coherence time, hence change of the field dependence. Therefore, we investigate the magnetoconductivity before and after CoPc decoration. The change of the conductivity with the magnetic field, $\Delta\sigma(B) = \sigma(B) - \sigma(0)$, is depicted in Fig. 2(a–f). A narrow dip appears around $B = 0$. This positive magnetoconductivity is the hallmark of weak localization. The functional form of the magnetoconductivity is determined by various scattering processes, which will be explained later. When only the phase coherence time varies, e.g., the curves at different temperatures and the same gate voltage, the narrower the dip, the longer the coherence time $\tau_\phi$ is. As temperature increases, the dip gradually fades out, as a result of reduction of $\tau_\phi$ due to electron-electron scattering.

Quantitative estimation of $\tau_\phi$ can be obtained by fitting the experiment data to an equation widely used to describe WL in graphene [39]:

$$\delta\sigma(B) = \frac{e^2}{\pi h}\left[F\left(\frac{B}{B_\phi}\right) - F\left(\frac{B}{B_\phi + 2B_i}\right) - 2F\left(\frac{B}{B_\phi + B_i + B_*}\right)\right]$$
$$F(z) = \ln(z) + \psi\left(\frac{1}{2} + \frac{1}{z}\right), B_{\phi,i,*} = \frac{\hbar}{4De\tau_{\phi,i,*}}, \quad (1)$$

where $\psi$ is the digamma function, $e$ the elementary charge, $\hbar$ the reduced Plank constant, $D$ the diffusion constant, $\tau_i$ the intervalley scattering time, and $\tau_*$ the intravalley scattering time. At low temperatures, universal conductance fluctuations appear and introduce some error to the fitting. The error diminishes as temperature increases because the fluctuations damp faster than the weak localization. By performing the fitting around the zero field, the effect can be further minimized, for the weak localization has a stronger field dependence that the fluctuations. $D$ is calculated from the conductivity. It is reasonable to assume that $\tau_i$

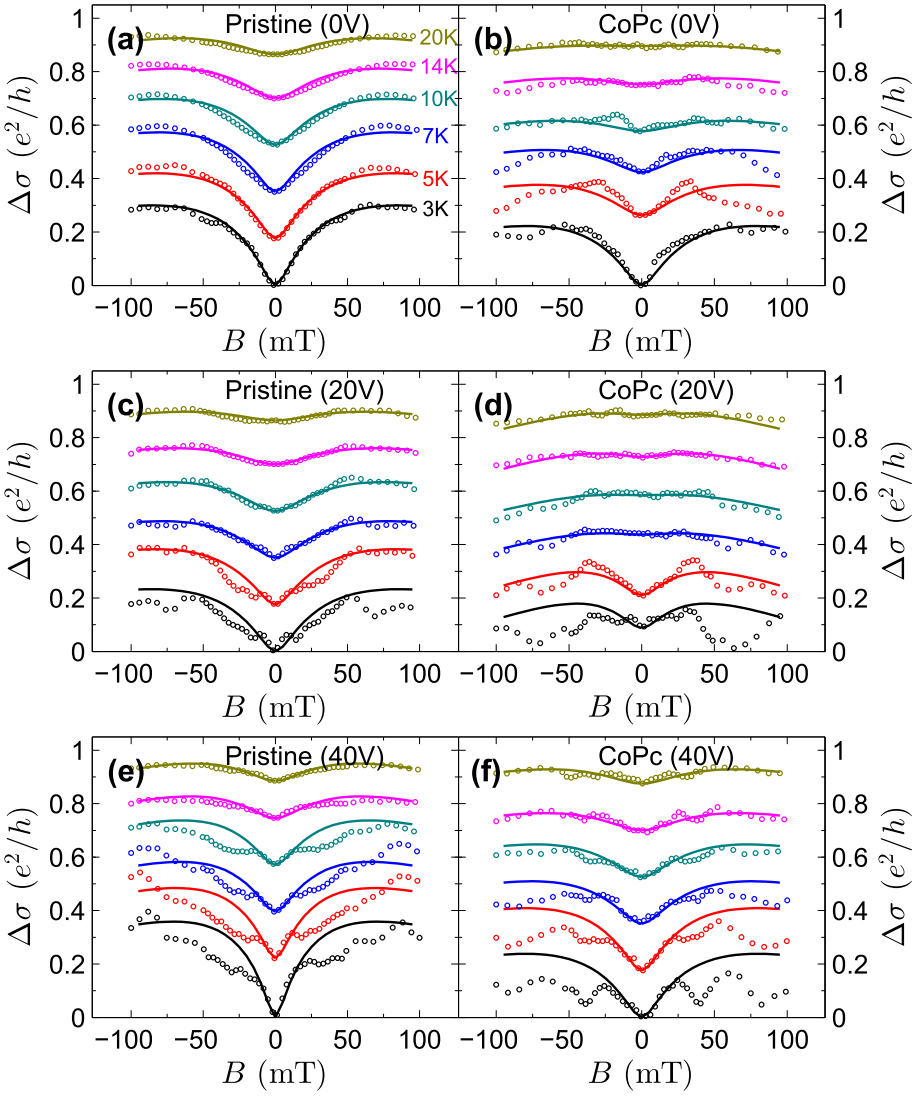


**Fig. 2.** Low field magnetoconductivity $\Delta\sigma$ at various temperatures from $T = 3$ K to 20 K. Data are shifted in $y$ for clarity. Solid lines are best fits of the experiment data around the dips (dotted line) to Eq. (1). Pristine graphene at $V_g = 0$ V (a), 20 V (c), 40 V (e) and CoPc decorated graphene at $V_g = 0$ V (b), 20 V (d), 40 V (f) are displayed.

and $\tau_*$ are independent of temperature, as they are caused by defects or warping of the energy band [39]. They are determined by fitting the low temperature curves and remain fixed for other temperatures [40,41].

The fitted parameter $\tau_\phi$ as a function of $T$ is plotted in Fig. 3. For pristine graphene, the inelastic scattering rate $1/\tau_\phi$ displays a $T$ linear dependence, consistent with previous studies [40–42]. The dependence indicates that electron-electron scattering is the dominant source for decoherence, while electron-phonon scattering is negligible. However, upon CoPc decoration, $1/\tau_\phi$ is enhanced at high temperatures, hence deviates from the linear dependence. The enhancement suggests additional source for phase decoherence. Similar additional decoherence source apart from electron-electron scattering has been observed in florinated graphene [24], which was attributed to spin-flip scattering. Thus, it is evident that CoPc molecules also induce spin-flip scattering. In this case, the decoherence rate consists of two contributions, $\tau_\phi^{-1} = \tau_{ee}^{-1} + \tau_{sf}^{-1}$, where $\tau_{ee}^{-1}$ is the electron-electron scattering rate, $\tau_{sf}$ the spin-flip scattering rate. The difference of $1/\tau_\phi$ between pristine and CoPc decorated graphene in Fig. 3 results from $1/\tau_{sf}$. It can be seen that the spin-flip scattering rate is negligible at low temperatures, while it increases with temperature. The onset temperature of the increase is higher at $V_g = 20$ V than $V_g = 0$ V. At $V_g = 40$ V, the increase remains insignificant for the whole temperature range. It is unlikely that the Kondo effect appears at low gate voltages and disappears at a higher gate voltage (higher density of states), as the effect should be enhanced by the density of state $\rho(E_F)$, $T_K \propto \exp -1/J\rho(E_F)$. It is thus inferred that the onset temperature at $V_g = 40$ V is even higher than 20 K. Note that there seems to be a positive deviation of the decoherence rate after decoration, particularly for $V_g = 40$ V. Although it might be related to the variation of the Kondo coupling originated from different adsorption sites or the orientation of the magnetic molecule [23,43,44], the deviation is too small to be certain.

We now show that this intriguing temperature and gate dependence agree well with the predicted Kondo screening in graphene [10,16]. It is known that the coupling between a local magnetic moment and itinerant electrons leads to screening of the local moment, which occurs below a characteristic temperature $T_K$, so-called Kondo temperature. As a result, the spin-flip scattering rate is depressed below $T_K$, which is observed in our experiment. The rate $1/\tau_{sf}$ goes as $T/T_K$ [45,46], so at sufficiently low temperature, it becomes negligible, which accounts for the overlap of $1/\tau_\phi$ at low temperatures between pristine and decorated graphene.

The Kondo temperature of graphene has been theoretically studied [10,16]. Away from the Dirac point, it has been estimated as $k_B T_K \sim \Delta$

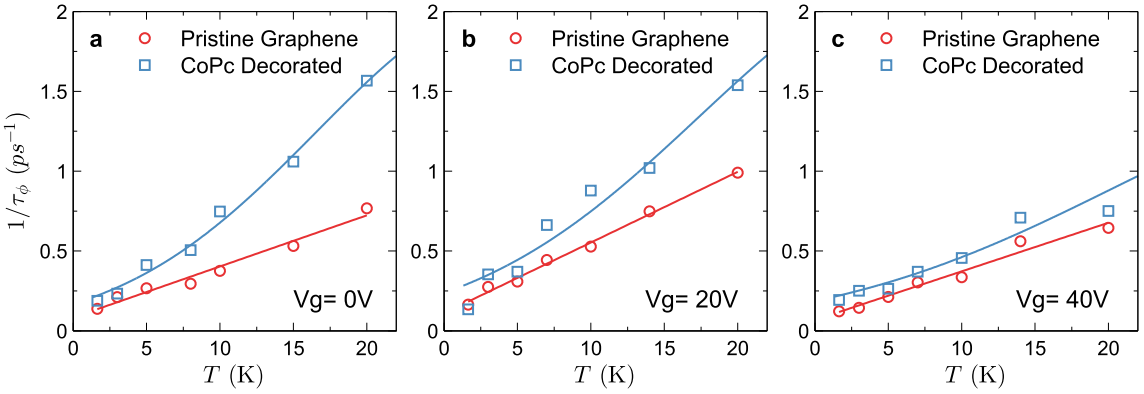


**Fig. 3.** Phase coherence time $\tau_\phi$ obtained by fitting are plotted as a function of temperature. (a) $V_g = 0$ V, (b) $V_g = 20$ V, (c) $V_g = 40$ V. Red circles represent pristine graphene, while blue squares represent CoPc decorated graphene. The red solid lines are best fits of experiment data to $1/\tau_\phi = 1/\tau_{ee} = \alpha \cdot T$, and the blue solid lines are guide to eyes. (For interpretation of the references to colour in this figure legend, the reader is referred to the Web version of this article.)

$\exp(-1/J\rho)$, where $\Delta$ is the band cutoff, $J$ the coupling energy, $\rho$ the density of states of graphene ($\rho \propto \sqrt{n} \propto \sqrt{V_g}$). Here, $n$ is the carrier concentration. Apparently, a higher gate voltage leads to a higher Kondo temperature, which is consistent with the gate dependence in Fig. 3. On the other hand, the Kondo effect at the Dirac point is expected to exhibit a rich phase diagram, depending on the coupling strength and the particle-hole symmetry, etc [10]. Unfortunately, our transport measurement is an average of all scattering events, so it suffers from variation of the Kondo coupling due to charge puddles and absorption geometries. We were not able to investigate these phases. Local probes, such as scanning tunneling microscopy, may reveal the intriguing physics at the Dirac point in this system in the future.

The mechanism for the tunable Kondo effect is illustrated in Fig. 4. When the carrier concentration is very low, the magnetic moment is poorly screened by electrons, leading to a strong spin-flip scattering. With increasing carrier concentration, the screening effect is enhanced, resulting in a weaker spin-flip scattering. At sufficiently high carrier concentration, the spin-flip scattering is substantially suppressed below 20 K, seen Fig. 4(c). The gate tunable Kondo effect provides us a new means to electrically control the spin decoherence. Although the interaction between electrons and the local moment in CoPc is evident, the spin scattering rate is considerably low considering a monolayer coverage. From the maximum spin-flip scattering rate observed at $V_g = 0$ V and $T = 20$ K, one can estimate the spin diffusion length, $l_s = \sqrt{(D\tau_s)} \sim 100$ nm, much larger than the distance between molecules (1.5 nm). We rule out an extremely weak coupling between electrons and local moments as the origin of the discrepancy, because Kondo screening, which depends not on the density of moment, but on the strength of the coupling [45], appears up to 20 K (Fig. 4(c)), suggesting a relatively strong coupling [47]. The above unique behavior of Kondo screening in graphene tallies with theories [16,31] and previous experiment [26]. Therefore, the plausible explanation is that only a very small fraction of these CoPc molecules forms a Kondo coupling to electrons in graphene. This is consistent with previous experiments which have indeed shown that the Kondo coupling depends on the adsorption site and the orientation of the magnetic molecule [23,43,44].

Another characteristic of the Kondo effect is a logarithmic temperature dependence in the resistivity [1]. However, this feature can often be obscured by other effects. For graphene on $SiO_2$, both electron-electron interaction [48] and weak localization [39]contribute a logarithmic temperature dependence, which makes it hard to identify the Kondo effect. Fortunately, contribution from these two effects can be

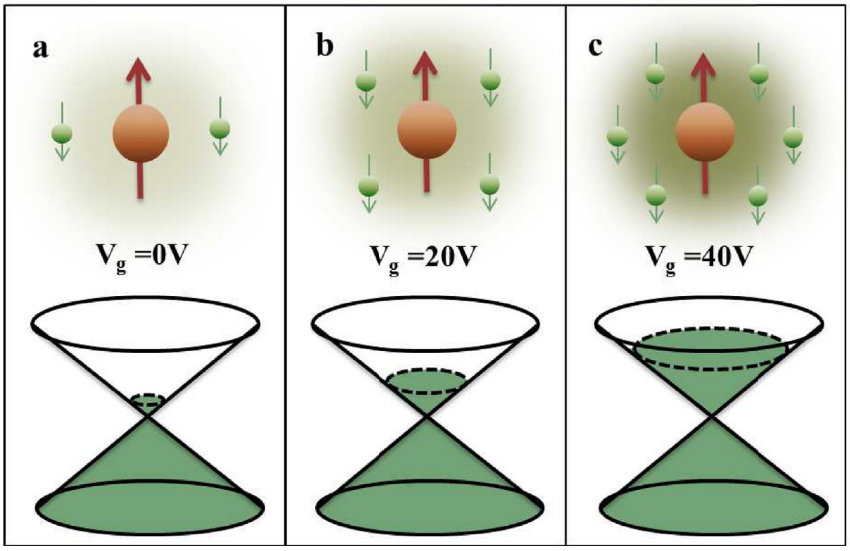


**Fig. 4.** Schematic diagram for density dependent screening of a magnetic moment in graphene. (a) Is at a very low carrier concentration with $V_g = 0$ V. (b) Is at a moderate concentration with $V_g = 20$ V. (c) Is at a high concentration with $V_g = 40$ V. The screening of the magnetic moment gets stronger with the increase of the carrier concentration.

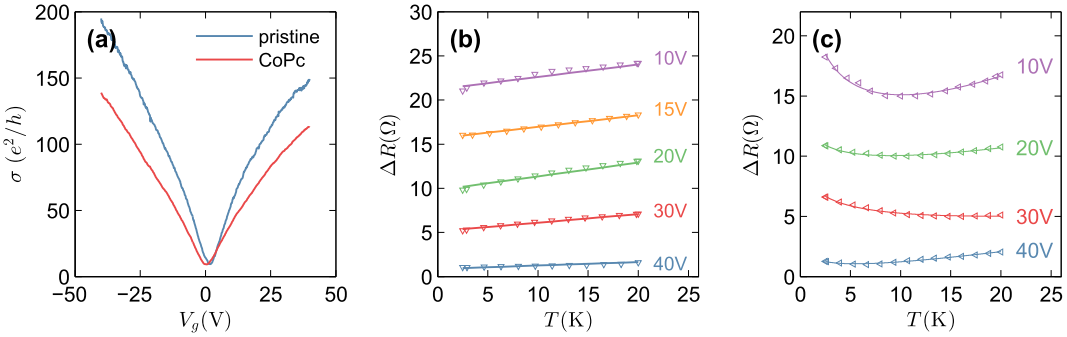


**Fig. 5.** (a) Conductivity versus gate voltage for pristine graphene/*h*-BN (blue line) and CoPc decorated graphene/*h*-BN (red line). A slight left shift of Dirac point(~1.5 V) is observed after decoration. Temperature dependence of resistivity at different gate voltage for pristine graphene/*h*-BN(b), and CoPc decorated graphene/*h*-BN(c) are measured. Pronounced upturn is observed after CoPc decoration. All the resistivity is calculated as $\Delta R = R(T) - \min\{R(T)\}$. The solid curves in (b) are best linear fits, and those in (c) are best fits to $\rho_0 + \rho_l T + \rho_K \ln(T)$. The curves are all shifted in *y* axis for clarity. (For interpretation of the references to colour in this figure legend, the reader is referred to the Web version of this article.)

greatly suppressed in graphene on hexagonal boron nitride crystals(*h*-BN) owing to much less disorder [42,48–50]. As a result, the emergence of a logarithmic temperature dependence in the resistivity alone can be seen as evidence for the Kondo effect.

Hence, we turn to investigate the temperature dependence of resistivity in graphene/*h*-BN device. The gate voltage dependence of resistivity is displayed in Fig. 5(a). The mobility of pristine graphene is high, about 22000 $cm^2/V{\cdot}s$. Because of the high quality of the device, no weak localization [39] was observed in magnetoresistance both before and after decoration (see Fig. S5 in the Supplementary Materials). Besides, the resistivity at various gate voltages decreases monotonically with decreasing temperature, which is in agreement with phonon scattering [51]. This further indicates the suppression of electron-electron interaction induced resistance. After CoPc molecule decoration, the mobility is reduced to 14000 $cm^2/V{\cdot}s$ and a slightly left shift of Dirac point ~1.5 V is observed. Intriguingly, a pronounced upturn of resistance emerges at low temperatures for different gate voltages, seen in Fig. 5(c). The non-monotonic behavior can be well fitted by a formula consisting of two contributions, *i.e.* a linear temperature dependence due to phonon scattering [51–53] and a logarithmic dependence. Since the weak localization, giving rise to a logarithmic component, is absent, the latter can be attributed to the Kondo effect. Although the Kondo effect is evident, its magnitude is merely 2% of the total increase of resistance after decoration(see Fig. 5(c)). This suggests that CoPc molecules give rise to far more normal scattering than Kondo scattering, which agrees with the previous phase coherence time analysis. Since $\tau_\phi$ is directly affected by the Kondo scattering, but not the mean free path, the phase coherence analysis is a more sensitive method for detection of the Kondo effect in this experiment. We did not perform quantitative analysis on the temperature dependence as the logarithmic contribution is very weak. Nevertheless, the logarithmic increase of the resistivity with decreasing temperature qualitatively corroborates with magnetoresistance results.

## 3. Conclusion

In conclusion, our experiment shows evidence of the Kondo effect in CoPc decorated graphene. By decreasing the carrier concentration, we have observed a strong suppression of Kondo screening inferred by an increase of spin-flip scattering. This is consistent with theoretical predictions of poor screening of local magnetic moments at the Dirac point. Our experiment demonstrates graphene as a highly tunable system for studying the Kondo physics. The ability to turn on/off Kondo screen also provides a means to electrically control the spin coherence, which may be useful in spintronics [32].

### 3.1. Methods

**Device Fabrication.** Monolayer graphene flakes were exfoliated from Kish graphite onto 285-nm $SiO_2$/Si substrates and identified by optical microscope(further confirmation by quantum hall effect, see Fig. S4). To obtain an ultra clean surface, a shadow mask method was used to fabricate graphene devices instead of the conventional e-beam lithography. Metallic contacts were made of 5 nm Pd/60 nm Au by e-beam deposition (see Fig. 1 (a), Fig. S2).

Graphene/*h*-BN device is fabricated by a dry transfer technique. Commercially available *h*-BN powder (Momentive, Polartherm grade PT110) is used for the mechanical cleavage. Firstly, graphene flakes and thin *h*-BN crystals were exfoliated separately onto 285-nm $SiO_2$/Si substrates. By optical and atomic force microscopy, we select *h*-BN crystals with thickness between 10 and 35 nm. For transfer, we prepare a transparent stamp, which consists of a 0.5 mm thick polydimethylsiloxane(PDMS) film spin-coated with a layer of polymethyl methacrylate(PMMA). The stamp is used to pick up graphene flakes on $SiO_2$ and release it onto *h*-BN crystals. A homemade micro-manipulator alignment system with a heating stage is employed for transfer. For this type of devices, a standard electron beam lithography technique is used for fabrication of electrodes.

***In-situ* Deposition.** CoPc was acquired from Sigma Aldrich ($\beta$-form, dye content = 97%). Each molecule consists of a $Co^{+2}$ at the center and a macrocycle of alternating carbon and nitrogen atoms [37,38], see the inset of Fig. 1(b). CoPc molecule decoration was performed in a dilution refrigerator with an *in-situ* thermal evaporator. The coverage is estimated by monitoring the resistance of the sample during deposition. Increasing the coverage of CoPc leads to a monotonically shift of the Dirac point to the negative gate voltage. Hence, if we measure the resistance at a fixed gate voltage (lower than initial Dirac point voltage), it will increase monotonically until about a monolayer coverage. Further deposition gives rise to no appreciable change of resistance and the Dirac point.

## Acknowledgements

This work was supported by National Key Basic Research Program of China (Project No.2013CBA01603, No.2016YFA0300600 and 2016YFA0300903) and NSFC (Project Nos. 11074007, 11774009, 11222436, 11234001 and 51522201). LZ thank the grant supported by Guangdong Innovative and Entrepreneurial Research Team Program (Project No. 2016ZT06D348) and Shenzhen Peacock Program (Project No. KQTD2016022619565991).

## Appendix A. Supplementary data

Supplementary data related to this article can be found at https://doi.org/10.1016/j.ssc.2018.05.001.

## References


[1] J. Kondo, Resistance minimum in dilute magnetic alloys, Prog. Theor. Phys. 32 (1) (1964) 37–49, https://doi.org/10.1143/PTP.32.37, http://ptp.oxfordjournals.org/content/32/1/37.full.pdf+html, http://ptp.oxfordjournals.org/content/32/1/37.abstract. arXiv.

[2] L. Kouwenhoven, L. Glazman, Revival of the Kondo effect, Phys. World 14 (1) (2001) 33–38, http://iopscience.iop.org/2058-7058.

[3] G.D. Scott, D. Natelson, Kondo resonances in molecular devices, ACS Nano 4 (7) (2010) 3560–3579. pMID: 20568709. arXiv: https://doi.org/10.1021/nn100793s.

[4] K. Wilson, Renormalization group - critical phenomena and Kondo problem, Rev. Mod. Phys. 47 (4) (1975) 773–840, https://doi.org/10.1103/RevModPhys.47.773.

[5] G.R. Stewart, Heavy-fermion systems, Rev. Mod. Phys. 56 (1984) 755–787, https://doi.org/10.1103/RevModPhys.56.755.

[6] J.J. Joyce, A.J. Arko, J. Lawrence, P.C. Canfield, Z. Fisk, R.J. Bartlett, J.D. Thompson, Temperature-invariant photoelectron spectra in cerium heavy-fermion compounds: inconsistencies with the Kondo model, Phys. Rev. Lett. 68 (1992) 236–239, https://doi.org/10.1103/PhysRevLett.68.236.

[7] A. Schröder, G. Aeppli, R. Coldea, M. Adams, O. Stockert, H. Löhneysen, E. Bucher, R. Ramazashvili, P. Coleman, Onset of antiferromagnetism in heavy-fermion metals, Nature 407 (6802) (2000) 351–355, http://www.nature.com/nature/journal/v407/n6802/abs/407351a0.html.

[8] A. Polkovnikov, S. Sachdev, M. Vojta, Impurity in a *d*-wave superconductor: Kondo effect and stm spectra, Phys. Rev. Lett. 86 (2001) 296–299, https://doi.org/10.1103/PhysRevLett.86.296.

[9] B. Lake, H. Rønnow, N. Christensen, G. Aeppli, K. Lefmann, D. McMorrow, P. Vorderwisch, P. Smeibidl, N. Mangkorntong, T. Sasagawa, et al., Antiferromagnetic order induced by an applied magnetic field in a high-temperature superconductor, Nature 415 (6869) (2002) 299–302, http://www.nature.com/nature/journal/v415/n6869/abs/415299a.html.

[10] L. Fritz, M. Vojta, The physics of Kondo impurities in graphene, Rep. Prog. Phys. 76 (3) (2013) 032501, https://doi.org/10.1088/0034-4885/76/3/032501.

[11] D. Jacob, G. Kotliar, Orbital selective and tunable Kondo effect of magnetic adatoms on graphene: correlated electronic structure calculations, Phys. Rev. B 82 (8) (2010) 085423, https://doi.org/10.1103/PhysRevB.82.085423.

[12] B. Uchoa, T.G. Rappoport, A.H.C. Neto, Kondo quantum criticality of magnetic adatoms in graphene, Phys. Rev. Lett. 106 (1) (2011) 016801, https://doi.org/10.1103/PhysRevLett.106.016801.

[13] M. Vojta, L. Fritz, R. Bulla, Gate-controlled Kondo screening in graphene: quantum criticality and electron-hole asymmetry, Europhys. Lett. 90 (2) (2010) 27006, https://doi.org/10.1209/0295-5075/90/27006.

[14] T.O. Wehling, S. Yuan, A.I. Lichtenstein, A.K. Geim, M.I. Katsnelson, Resonant scattering by realistic impurities in graphene, Phys. Rev. Lett. 105 (2010) 056802, https://doi.org/10.1103/PhysRevLett.105.056802.

[15] M. Kharitonov, G. Kotliar, Kondo effect in monolayer and bilayer graphene: physical realizations of the multichannel Kondo models, Phys. Rev. B 88 (2013) 201103, https://doi.org/10.1103/PhysRevB.88.201103.

[16] K. Sengupta, G. Baskaran, Tuning Kondo physics in graphene with gate voltage, Phys. Rev. B 77 (2008) 045417, https://doi.org/10.1103/PhysRevB.77.045417.

[17] P.-W. Lo, G.-Y. Guo, F.B. Anders, Gate-tunable Kondo resistivity and dephasing rate in graphene studied by numerical renormalization group calculations, Phys. Rev. B 89 (2014) 195424, https://doi.org/10.1103/PhysRevB.89.195424.

[18] A.H. Castro Neto, F. Guinea, N.M.R. Peres, K.S. Novoselov, A.K. Geim, The electronic properties of graphene, Rev. Mod. Phys. 81 (2009) 109–162, https://doi.org/10.1103/RevModPhys.81.109.

[19] K. Novoselov, A.K. Geim, S. Morozov, D. Jiang, M.K.I. Grigorieva, S. Dubonos, A. Firsov, Two-dimensional gas of massless Dirac fermions in graphene, Nature 438 (7065) (2005) 197–200, http://www.nature.com/nature/journal/v438/n7065/abs/nature04233.html.

[20] D. Withoff, E. Fradkin, Phase transitions in gapless fermi systems with magnetic impurities, Phys. Rev. Lett. 64 (1990) 1835–1838, https://doi.org/10.1103/PhysRevLett.64.1835.

[21] S. Omar, M. Gurram, I.J. Vera-Marun, X. Zhang, E.H. Huisman, A. Kaverzin, B.L. Feringa, B.J. van Wees, Spin relaxation in graphene with self-assembled cobalt porphyrin molecules, Phys. Rev. B 92 (2015) 115442, https://doi.org/10.1103/PhysRevB.92.115442.

[22] F. Donati, L. Gragnaniello, A. Cavallin, F.D. Natterer, Q. Dubout, M. Pivetta, F. Patthey, J. Dreiser, C. Piamonteze, S. Rusponi, H. Brune, Tailoring the magnetism of co atoms on graphene through substrate hybridization, Phys. Rev. Lett. 113 (2014) 177201, https://doi.org/10.1103/PhysRevLett.113.177201.

[23] J. Ren, H. Guo, J. Pan, Y.Y. Zhang, X. Wu, H.-G. Luo, S. Du, S.T. Pantelides, H.-J. Gao, Kondo effect of cobalt adatoms on a graphene monolayer controlled by substrate-induced ripples, Nano Lett. 14 (7) (2014) 4011–4015. pMID: 24905855. arXiv: https://doi.org/10.1021/nl501425n.

[24] X. Hong, K. Zou, B. Wang, S.-H. Cheng, J. Zhu, Evidence for spin-flip scattering and local moments in dilute fluorinated graphene, Phys. Rev. Lett. 108 (22) (2012) 226602, https://journals.aps.org/prl/abstract/10.1103/PhysRevLett.108.226602.

[25] V.W. Brar, R. Decker, H.-M. Solowan, Y. Wang, L. Maserati, K.T. Chan, H. Lee, C.O. Girit, A. Zettl, S.G. Louie, M.L. Cohen, M.F. Crommie, Gate-controlled ionization and screening of cobalt adatoms on a graphene surface, Nat. Phys. 7 (1) (2011) 43–47, https://doi.org/10.1038/nphys1807.

[26] J.-H. Chen, L. Li, W.G. Cullen, E.D. Williams, M.S. Fuhrer, Tunable Kondo effect in graphene with defects, Nat. Phys. 7 (7) (2011) 535, https://doi.org/10.1038/nphys1962.

[27] L. Kou, C. Tang, W. Guo, C. Chen, Tunable magnetism in strained graphene with topological line defect, ACS Nano 5 (2) (2011) 1012–1017. pMID: 21229964. arXiv: https://doi.org/10.1021/nn1024175.

[28] N. Leconte, D. Soriano, S. Roche, P. Ordejon, J.-C. Charlier, J.J. Palacios, Magnetism-dependent transport phenomena in hydrogenated graphene: from spin-splitting to localization effects, ACS Nano 5 (5) (2011) 3987–3992. pMID: 21469688. arXiv: https://doi.org/10.1021/nn200558d.

[29] V.M. Pereira, F. Guinea, J.M.B. Lopes dos Santos, N.M.R. Peres, A.H. Castro Neto, Disorder induced localized states in graphene, Phys. Rev. Lett. 96 (2006) 036801, https://doi.org/10.1103/PhysRevLett.96.036801.

[30] F. Banhart, J. Kotakoski, A.V. Krasheninnikov, Structural defects in graphene, ACS Nano 5 (1) (2011) 26–41, https://doi.org/10.1021/nn102598m.

[31] M. Hentschel, F. Guinea, Orthogonality catastrophe and Kondo effect in graphene, Phys. Rev. B 76 (2007) 115407, https://doi.org/10.1103/PhysRevB.76.115407.

[32] J. Igor, S. Fabian, Sarma Das, Spintronics: fundamentals and applications, Rev. Mod. Phys. 76 (2004) 323–410, https://doi.org/10.1103/RevModPhys.76.323.

[33] B. Yan, Q. Han, Z. Jia, J. Niu, T. Cai, D. Yu, X. Wu, Electrical control of intervalley scattering in graphene via the charge state of defects, Phys. Rev. B 93 (2016) 041407, https://doi.org/10.1103/PhysRevB.93.041407.

[34] S.K. Hinen, M. Stepanova, R. Drost, P. Liljeroth, J. Lahtinen, J. Sainio, Self-assembly of cobalt-phthalocyanine molecules on epitaxial graphene on ir(111), J. Phys. Chem. C 116 (38) (2012) 20433–20437. arXiv: https://doi.org/10.1021/jp306439h.

[35] M.-S. Liao, S. Scheiner, Electronic structure and bonding in metal phthalocyanines, metal=fe, co, ni, cu, zn, mg, J. Chem. Phys. 114 (22) (2001) 9780–9791, https://doi.org/10.1063/1.1367374.

[36] K. Teichmann, M. Wenderoth, S. Loth, R.G. Ulbrich, J.K. Garleff, A.P. Wijnheijmer, P.M. Koenraad, Controlled charge switching on a single donor with a scanning tunneling microscope, Phys. Rev. Lett. 101 (2008) 076103, https://doi.org/10.1103/PhysRevLett.101.076103.

[37] S. Kremer, W. Henke, D. Reinen, High-spin-low-spin equilibriums of cobalt (2+) in the terpyridine complexes co (terpy) 2x2. nh2o, Inorg. Chem. 21 (8) (1982) 3013–3022, http://pubs.acs.org/doi/pdf/10.1021/ic00138a019.

[38] T. Gang, M.D. Yilmaz, D. Atac, S.K. Bose, E. Strambini, A.H. Velders, M.P. de Jong, J. Huskens, W.G. van der Wiel, Tunable doping of a metal with molecular spins, Nat. Nanotechnol. 7 (4) (2012) 232–236, https://doi.org/10.1038/NNANO.2012.1, http://www.nature.com/nnano/journal/v7/n4/full/nnano.2012.1.html.

[39] E. McCann, K. Kechedzhi, V.I. Fal'ko, H. Suzuura, T. Ando, B.L. Altshuler, Weak-localization magnetoresistance and valley symmetry in graphene, Phys. Rev. Lett. 97 (2006) 146805, https://doi.org/10.1103/PhysRevLett.97.146805.

[40] X.S. Wu, X. Li, Z. Song, C. Berger, W.A. de Heer, Weak antilocalization in epitaxial graphene: evidence for chiral electrons, Phys. Rev. Lett. 98 (13) (2007) 136801, https://journals.aps.org/prl/abstract/10.1103/PhysRevLett.98.136801.

[41] F.V. Tikhonenko, D.W. Horsell, R.V. Gorbachev, A.K. Savchenko, Weak localization in graphene flakes, Phys. Rev. Lett. 100 (2008) 056802, https://doi.org/10.1103/PhysRevLett.100.056802.

[42] S.V. Morozov, K.S. Novoselov, M.I. Katsnelson, F. Schedin, L.A. Ponomarenko, D. Jiang, A.K. Geim, Strong suppression of weak localization in graphene, Phys. Rev. Lett. 97 (2006) 016801, https://doi.org/10.1103/PhysRevLett.97.016801.

[43] L. Liu, K. Yang, Y. Jiang, B. Song, W. Xiao, L. Li, H. Zhou, Y. Wang, S. Du, M. Ouyang, et al., Reversible single spin control of individual magnetic molecule by hydrogen atom adsorption, Sci. Rep. 3 (2013) 1210, http://www.nature.com/srep/2013/130204/srep01210/full/srep01210.html?message-global=remove&WT.ec_id=SREP-20130205.

[44] Q. Zhang, G. Kuang, R. Pang, X. Shi, N. Lin, Switching molecular Kondo effect via supramolecular interaction, ACS Nano 9 (12) (2015) 12521–12528. pMID: 26568262. arXiv: https://doi.org/10.1021/acsnano.5b06120.

[45] C.V. Haesendonck, J. Vranken, Y. Bruynseraede, Resonant Kondo scattering of weakly localized electrons, Phys. Rev. Lett. 58 (1987) 1968–1971, https://doi.org/10.1103/PhysRevLett.58.1968.

[46] T. Micklitz, A. Altland, T.A. Costi, A. Rosch, Universal dephasing rate due to diluted Kondo impurities, Phys. Rev. Lett. 96 (2006) 226601, https://doi.org/10.1103/PhysRevLett.96.226601.

[47] M. Serri, W. Wu, L.R. Fleet, N.M. Harrison, C.F. Hirjibehedin, C.W. Kay, A.J. Fisher, G. Aeppli, S. Heutz, High-temperature antiferromagnetism in molecular semiconductor thin films and nanostructures, Nat. Commun. 5 (2014) 3079, https://doi.org/10.1038/ncomms4079.

[48] B.L. Altshuler, A.G. Aronov, P.A. Lee, Interaction effects in disordered fermi systems in two dimensions, Phys. Rev. Lett. 44 (1980) 1288–1291, https://doi.org/10.1103/PhysRevLett.44.1288.

[49] C. Dean, A. Young, I. Meric, C. Lee, L. Wang, S. Sorgenfrei, K. Watanabe, T. Taniguchi, P. Kim, K. Shepard, et al., Boron nitride substrates for high-quality graphene electronics, Nat. Nanotechnol. 5 (10) (2010) 722–726, http://www.nature.com/nnano/journal/v5/n10/full/nnano.2010.172.html.

[50] A.A. Kozikov, A.K. Savchenko, B.N. Narozhny, A.V. Shytov, Electron-electron interactions in the conductivity of graphene, Phys. Rev. B 82 (2010) 075424, https://doi.org/10.1103/PhysRevB.82.075424.

[51] J.-H. Chen, C. Jang, S. Xiao, M. Ishigami, M.S. Fuhrer, Intrinsic and extrinsic performance limits of graphene devices on sio2, Nat. Nanotechnol. 3 (4) (2008) 206–209, http://www.nature.com/nnano/journal/v3/n4/abs/nnano.2008.58.html.

[52] S.V. Morozov, K.S. Novoselov, M.I. Katsnelson, F. Schedin, D.C. Elias, J.A. Jaszczak, A.K. Geim, Giant intrinsic Carrier mobilities in graphene and its bilayer, Phys. Rev. Lett. 100 (2008) 016602, https://doi.org/10.1103/PhysRevLett.100.016602.

[53] K. Bolotin, K. Sikes, Z. Jiang, M. Klima, G. Fudenberg, J. Hone, P. Kim, H. Stormer, Ultrahigh electron mobility in suspended graphene, Solid State Commun. 146 (9–10) (2008) 351–355, https://doi.org/10.1016/j.ssc.2008.02.024, http://www.sciencedirect.com/science/article/B6TVW-4S0JN2G-1/2/544b4113011a73221f4d3f2e368af79d.